

SURFACE CHARACTERIZATION OF RED MAPLE STRANDS AFTER HOT WATER EXTRACTION

Juan Jacobo Paredes[†]

Graduate Research Assistant

Ryan Mills[†]

Graduate Research Assistant

Stephen M. Shaler^{*†}

Associate Director

Douglas J. Gardner[†]

Professor of Wood Science

Advanced Engineered Wood Composites Center (AEWC)

Adriaan van Heiningen

Professor of Chemical Engineering

Department of Chemical and Biological Engineering

University of Maine

Orono, ME 04469

(Received September 2008)

Abstract. The conversion of carbohydrates from wood to make biofuels such as ethanol is a topic of widespread interest. A promising approach is the removal of the hemicellulosic wood component by extraction with subsequent conversion to biofuels while continuing to produce forest products. The impact of extraction on wood strands for use in strand-based composites was investigated. One tree of red maple (*Acer rubrum* L.) was used to create strands 10.2 cm long with a thickness of 0.9 mm. Three hot water extraction procedures at 160°C, corresponding to severity factors (SF) of 2.71, 3.54, and 3.81, were used resulting in an average weight loss of 5.7, 16.9 and 18.1%, respectively. Scanning electron microscopic imaging of selected wood strands showed that pores in the cell wall increased as SF increased. The distribution and size of the cell-wall pore structure showed up to a 22.2% increase. The sessile drop method, using distilled water, diiodomethane, and ethylene glycol, indicated more pronounced liquid wetting and penetration as SF increased. Inverse gas chromatography led to the finding that dispersive surface-free energy and acid-base characteristics increase with SF. The extraction procedures should be kept below a SF of 3.54 to minimize changes in adhesion performance.

Keywords: Hot water extraction, weight loss, porosity, contact angle, surface energy.

INTRODUCTION

Several procedures are available to extract hemicelluloses from wood, including acid prehydrolysis (Carrasco and Roy 1992), autohydrolysis (Lora and Wayman 1980), steam explosion developed in 1925 by W. H. Mason for hardboard production (Jeoh 1998), enzymatic hydrolysis

(Sjöström 1993), and hot water preextraction or a hydrothermal process (Garrote et al 1999; Yoon et al 2006). As wood is progressively heated, the results are 1) weight loss and 2) loss of bound water and water-soluble extractives (Stamm et al 1946; Seborg et al 1953; Hill 2006; Jara et al 2006). The presence of water or steam results in the formation of organic acids derived mostly from hemicelluloses that influence the production of cellular breakdown products (Mitchell 1988). Jara et al (2006)

* Corresponding author: shaler@maine.edu

† SWST member

reported that the compounds removed from red maple by hot water extraction had a higher percent of hemicelluloses than lignin and extractives. The hemicelluloses have the ability to be fermented into ethanol (Badger 2002; Fujita et al 2002). The remaining material, mostly cellulose and lignin, can be used to manufacture other wood products such as pulp (Mao et al 2008), OSB, and particle board.

The logical location for hot water extraction to take place in OSB manufacture would be between the strander and dryer. The pressurized conditions would significantly increase strand MC to near fully saturated conditions. This would create the need for process water in an OSB/OSL facility. The extract needs to be concentrated before fermentation (Dahlman et al 2007; Wood et al 2008). If that concentration occurred at the mill, it could reduce water requirements. Increased energy would also be required for drying, although significant amounts of moisture may be flashed off as the strands exit the extraction unit at high temperature. The costs associated with these operations along with capital costs would need to be offset by revenue from the sale of the extract and cost savings in other portions of the production process (eg VOC control).

In an earlier evaluation of the physical and mechanical properties of OSB produced from hot water-extracted material (Paredes et al 2008), it was shown that extraction resulted in a significant decrease from 807 to 260 kPa in internal bond strength (IB) while maintaining flexural performance at up to 17% weight loss. IB is often used to assess adhesion quality in OSB. Similar results were found by Bengtsson et al (2003) when glulam specimens made from heat-treated wood bonded using phenol-resorcinol-formaldehyde or polyvinylacetate was tested. It is known that heat and moisture cause changes in the wood structure by oxidation and decomposition of wood polymers influencing the wettability of wood (Varga and van der Zee 2008).

Contact angle, surface energy, porosity, and microstructure evaluation can be used for

understanding the wetting process between the wood strands and different liquid materials. Contact angle and surface-free energy information help to estimate the work of adhesion at the interface between wood and other materials (Gardner et al 1991; Lee et al 2007; Mills et al 2008). This investigation was undertaken to elucidate changes in the cell-wall structure and surface energies, which may have contributed to the lowering of adhesion strength.

EXPERIMENTAL PROCEDURE

Hot Water Extraction of Wood

One red maple (*Acer rubrum* L.) tree, 16.4 m height and 24.4 cm dia, was felled and debarked. A 1.2 m butt log was used to create 10 cm strands with a target thickness of 0.9 ± 0.05 mm using a 122 cm dia ring strander. After stranding, the material was conditioned at 38°C and 60% RH for 5 days in a dehumidification kiln until constant weight was attained. This was necessary to determine the correct amount of water to be added (see the following section). The average MC of the strands was 10.1% determined using a moisture balance.

A reactor was used for hot water extraction. The strands (500 g) were placed inside a high-pressure vessel filled with sufficient fresh water (tap water) to obtain a liquid–solid weight ratio of 4. The three extraction protocols involved heating from room temperature to 160°C in 50 min (preheating time) followed by constant temperature exposure times of 0, 45, or 90 min. Three replicate runs were made for each extraction condition. These extraction conditions were equated to a severity factor (SF) through the use of Eq 1 (Overend and Chornet 1987; Mosier et al 2002).

$$SF = \log_{10} \left(\int_0^t \left[\frac{T_r - T_b}{14.75} \right] dt \right) \quad (1)$$

where t is the residence time (min), T_r is the reaction temperature (°C), and T_b is the base temperature of 100°C. The energy of activation (14.75 kJ/kg/mol) assumes that the overall

process is hydrolytic and the overall conversion is first order (Overend and Chornet 1987; Jeoh 1998; Mosier et al 2002). Using Eq 1, SF of 2.71, 3.54, and 3.81 were calculated for the 0 (preheating time), 45, and 90 min extraction times, respectively. Strand weight loss (WL) as a result of the extraction process was determined by freeze drying the extracted liquid at a temperature of -42°C and between 1.3 and 1.5 GPa vacuum.

After the extraction, scanning electron micrographs revealed that material had been deposited on the wood surface (Fig 1a). Individual strands, including the control, were submerged in acetone (100%) for 3 min until they were completely saturated, placed in a beaker, and a vacuum was applied for approximately 2 h to wash out the extractive depositions (Fig 1b).

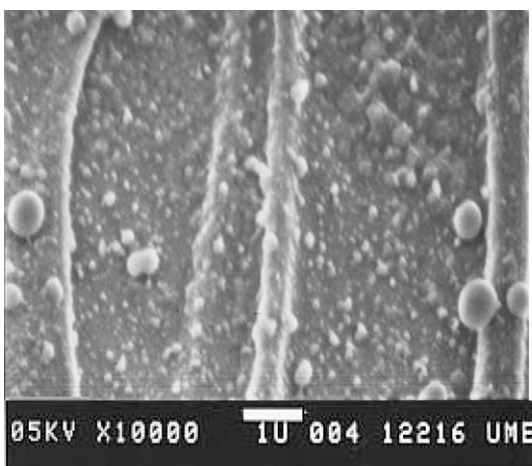
Microstructure Determination

Three specimens were randomly selected from each severity factor and the control (SF = 0). After specimen selection, 2×3 mm pieces were carefully trimmed with a razor blade and microscopically viewed to verify that no wood structure was damaged because of the preparation. A metal stud was covered with carbon

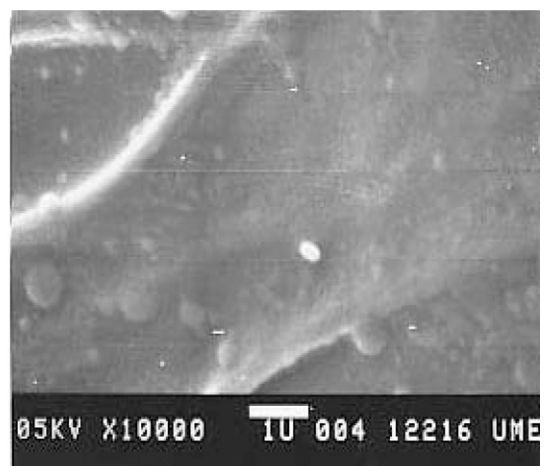
film and two specimens mounted, one showing the cross-section and the other the transverse section, a mixture of tangential and radial cut. Specimens were sputter-coated with a 40 nm gold layer. To minimize electron beam damage, an accelerating voltage of 5 keV was used while imaging with a scanning electron micrograph (SEM).

Porosity

The removal of cell-wall material by the extraction process was expected to influence the intracell-wall architecture. One way to measure the intracell-wall void structure is by mercury porosimetry (Blankenhorn et al 1978; Klose and Schinkel 2002; Moura et al 2005; Grioui et al 2007). Mercury porosimetry is suitable for many materials with pores in the approximate circular diameter range of $0.003 - 400 \mu\text{m}$, but it also works well in the range of $0.1 - 100 \mu\text{m}$ (ISO/AWI 2004). One of the limitations of the porosimeter is the difficulty to detect pores with diameters under $0.007 \mu\text{m}$ (Moura et al 2005). Samples were randomly selected from each severity factor and the control condition (unextracted). Ten sample replicates of each treatment were trimmed to a 25.4 mm dia, oven-dried, and grouped together for single



(a)



(b)

Figure 1. Side view of red maple vessel elements illustrating: (a) deposition of extracted substances after extraction (SF 3.81) and (b) subsequent view after removal of deposits by acetone wash. Scale bar = $1 \mu\text{m}$. SF = severity factor.

placement in the instrument vessel. The evaluation of pore size distribution was carried out according to ISO/AWI 15901-1. The pressure associated with measured mercury intrusion volume was related with pore size by the Washburn equation (Washburn 1921):

$$r = \frac{-2\gamma \cos \theta}{P} \quad (2)$$

where P is the imposed pressure (kPa), γ is the mercury surface tension (485 mJ/m²), θ is the contact angle (°), and r is the pore radius (μm). The cumulative volume was expressed as L/kg by normalizing the total mercury intrusion volume against the sample weight. The incremental intrusion volume was calculated by subtracting the cumulative volume, V_i measured at pressure P_i , from the cumulative volume V_{i+1} , measured at a higher pressure P_{i+1} , and was also adjusted for original wood weight. An approximate conversion from intrusion volume to cell-wall void volume can be made by dividing the normalized mercury volume by the cell-wall density (1500 kg/m³). The advancing and receding contact angle was assumed to be 130.0°, the filling pressure 4 kPa, and the final pressure 170 kPa with an equilibrium time of 10 s.

Cellulose Crystallinity

Wood strands were randomly selected from the three severity factors and the control (12 specimens). Individual samples of 25.4 × 25.4 × 0.9 mm were scanned with symmetric θ -2 θ Bragg-Brentano scattering geometry. The θ -2 θ diffraction scans were performed using a graded multilayer parabolic X-ray mirror and 0.18° parallel-plate collimator in quasiparallel beam geometry. The step size was 0.1 mm with a total range of 5 – 32°. Peaks were fitted to the scans using the program Profile Fit (Panalytical, the Netherlands, 1999, version 1.0C). The integrated areas of the fitted peaks were used to determine percent crystallinity according to previously described methods (Howell et al 2007). Cross-sectional width of the microfibril, related to the diagonal crystalline

regions, was determined using the Scherrer formula (Eq 3).

$$X_s = \frac{0.9\lambda}{B \cos \theta} \quad (3)$$

where X_s is width (nm), λ is the wavelength of the X-ray source (0.1541 nm), B is the full width at half maximum of the peak (rad), and θ the angle between the source and the sample (rad). Rietveld analysis was also performed to verify the results.

Contact Angle

Contact angle was determined using a sessile drop technique in which a drop of a known liquid is placed on the surface of a solid. It is assumed that the solid is perfectly smooth, rigid, isotropic, and that the liquid does not chemically react with the solid. Drop size is usually small to allow flowing and equilibration on the surface (Pocius 2002). However, porous materials such as wood exhibit a dynamic contact angle resulting from the interactions across the two interfaces as liquid/vapor meets the solid surface (wood).

Three different liquids were placed on the surface of the wood samples (single OSB strands). All measurements were conducted in a closed and narrow glass compartment kept at room temperature ($\pm 2^\circ\text{C}$) to minimize liquid loss by evaporation. Every sample was illuminated from the top using a light source equipped with a heat-absorbing filter at about 400 mm. The probe liquids were distilled water, diiodomethane, and ethylene glycol. A 5 μL drop size was used. Twelve replicates (drops) are performed for every liquid/substrate combination. Each drop was allowed to flow on the surface (3 s) before imaging. Digital images were analyzed to determine the contact angle of each drop.

Surface Energy

Wood material representing the three SF and the control were ground using a Wiley mill and then size-fractionated through a 60 mesh

screen producing a powder. Inverse gas chromatography (IGC) columns were packed with the powder and then conditioned at 103°C in the IGC with 15 mL of helium until the flame ionizing detector recorded a background signal of less than 5 pA at 30°C. The experiments were conducted using a fully automated Surface Measurements Systems SMS IGC (Alperton, UK) with head-space temperature control. Custom silane-treated glass tubes were used at temperatures of 30, 35, and 40°C at a flow rate of 15 mL/min. Vapors of high-performance liquid chromatography-grade polar and nonpolar probes were sampled by microsyringe, and an infinite dilute concentration of probe was injected into the packed column with the retention time measured by a flame ionization detector. An infinitely dilute sample of methane was injected to determine the dead time in the column. The probe and methane retention time were used with the mass of the packed material in the column for calculating the dispersive energy and Ka and Kb of the samples by the Schultz/Lavielle method (Lavielle and Schultz 1991). Calculations were performed using an Excel spreadsheet (Microsoft, Redmond, WA) and packaged software from SMS. To calculate Ka and Kb , Gutmann's equation, $-\Delta H_A^{AB} = Ka*DN + Kb$, is written in $y = mx + b$ form and

AN^* used where AN^* is in energy/mole because AN is a unitless value (Mills et al 2008):

$$\frac{-\Delta H_A^{AB}}{4.184AN^*} = \frac{DN}{AN^*}Ka + Kb \quad (4)$$

where DN and AN are the acceptor and donator numbers related to chemical references.

RESULTS AND DISCUSSION

Hot Water Extraction

As anticipated, WL increased with extraction time (Fig 2a). The WL was $5.7 \pm 0.3\%$, $16.6 \pm 0.8\%$, and $17.3 \pm 0.8\%$ for SF 2.71, 3.54, and 3.81, respectively. Using a one-way analysis of variance procedure, WL was found to be significantly influenced by extraction time ($p = 0.0001$). A Bonferroni multiple comparisons, at the 95.0% confidence level, indicated no significant difference between SF 3.54 and 3.81 conditions. As shown in Fig 1a, the wood surface of extracted material exhibited depositions of extract that were acetone-soluble. The question then was whether deposition of removed cell-wall material onto the cell wall biased the gross WL determinations. WL of the acetone-extracted strands was determined and the relationship of extraction conditions with

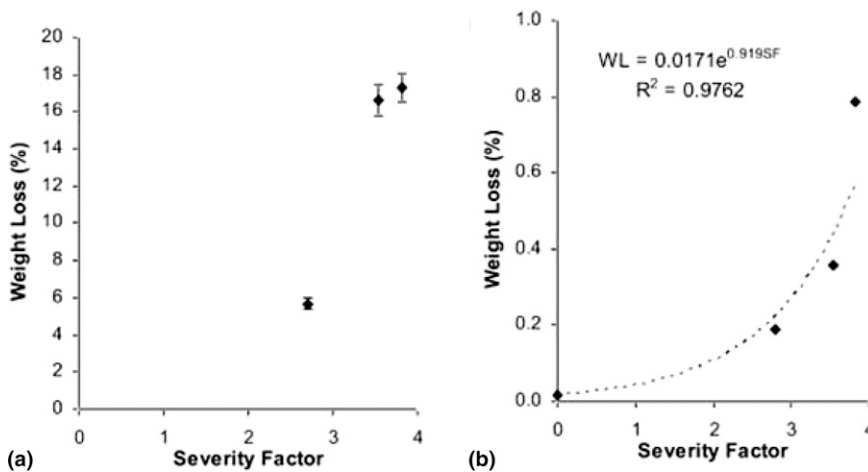


Figure 2. (a) The effect of time extraction on hydrothermal weight mass loss (%) of red maple and (b) changes in weight loss (%) of strands after an acetone wash showing exponential increase with increasing severity factor.

acetone washing WL was calculated (Fig 2b). An exponential relationship between acetone-soluble extract and WL was obtained with approximately 0.2, 0.4, and 0.8% WL attributed to SF 2.71, 3.54, and 3.81 conditions, respectively.

Depositions are thought to be attributed to self-assembly processes of polymers in aqueous solutions because of the presence of hydrophobic groups on the hydrophilic main chain (Akiyoshi et al 1993; Cochin et al 2001). Lignin itself shows agglomeration phenomena in aqueous solutions, and when the temperature was increased, it results in greater aggregations (Falkehag 1975; Norgren et al 2002). Westbye et al (2007) proposed an agglomeration mechanism for lignin-rich xylan fractions in aqueous solutions, suggesting that xylans play an active role in these aggregation phenomena. Thus, it is likely that the depositions found were aggregations of lignin and xylan that were produced during hot water extraction.

As wood is heated, the production of acetic and formic acid from hemicelluloses occurs by cellular breakdown, resulting in a loss of hemicelluloses, lignin, constitution water, and volatile extractives (Hill 2006; Jara et al 2006; Borrega and Karenlampi 2008). Also, 4-*O*-methylglucuronic and galacturonic acid can be formed during the hydrolysis of wood (Sundqvist et al 2006). Acetic acid is formed when acetyl groups split off as a result of wood degradation under severe hydrothermal conditions (Hill 2006; Sundqvist et al 2006). Water-soluble extracts from *Pinus radiata* MDF pulp indicated an acetylation of glucomannan components but no cellulose liberation (McDonald et al 1999). Jara et al (2006) found that arabinan, galactan, and mannan were the hemicelluloses most extracted at a low SF of 2.8, but when the SF increases, arabinan begins to degrade. Xylan is the most abundant hemicelluloses in red maple (Sjöström 1993), and this pentose sugar begins to be removed after a SF of 3.3, extracting a significant portion, 65% on original sugar, until a SF of 3.7 (Jara et al 2006).

After the hot water preextraction, the natural wood color changed from light yellow to more intense reddish brown during hydrothermal processing as a result of degradation of hemicelluloses, lignin, and certain extractive compounds (Sundqvist and Morén 2002). The most intense reddish brown occurred at the highest SF of 3.84; at low SF, color change also occurred. That is a commonly observed phenomenon in cooking; Maillard-Amodori mechanisms suggest that the presence of amino acids, reduced sugars, lignin, and tannins can result in the formation of colored compounds after chemical reaction as a result of heating (McDonald et al 2000).

Microstructure and Porosity

Cross-section. A micrograph set of control and SF 3.81 specimens is shown (Fig 3). Inspection of the cross-sections indicates that the pressurized hot water extraction did not induce cellular collapse. Some cell-wall scratches were present. These features are consistent with damage caused by the razor blade during specimen preparation.

Transverse evaluation. A transverse section of the control, SF 2.71, SF 3.54, and SF 3.81 materials clearly document damage to the cell wall as the extraction conditions became more severe (Fig 4). This damage was in the form of voids that increase in number as the extraction severity increases. The size of the voids and extent of their penetration within the cell wall cannot be determined using SEM. Previous analysis of the chemical composition of the material removed by the extraction process indicated that a negligible amount of cellulose was removed and that the dominant hemicellulose removed was xylan (Jara et al 2006). One assumes that the removed hemicellulose/lignin complex follows those locations in the cell wall as proposed by various researchers (Fengel and Wegener 1984; Lawoko et al 2004).

Cell-wall porosity. Pore volume and pore size distribution measurements were performed using mercury porosimetry (ISO/AWI 15901-1) assuming the pore structure is cylindrical and that the mercury is a nonwetting liquid that

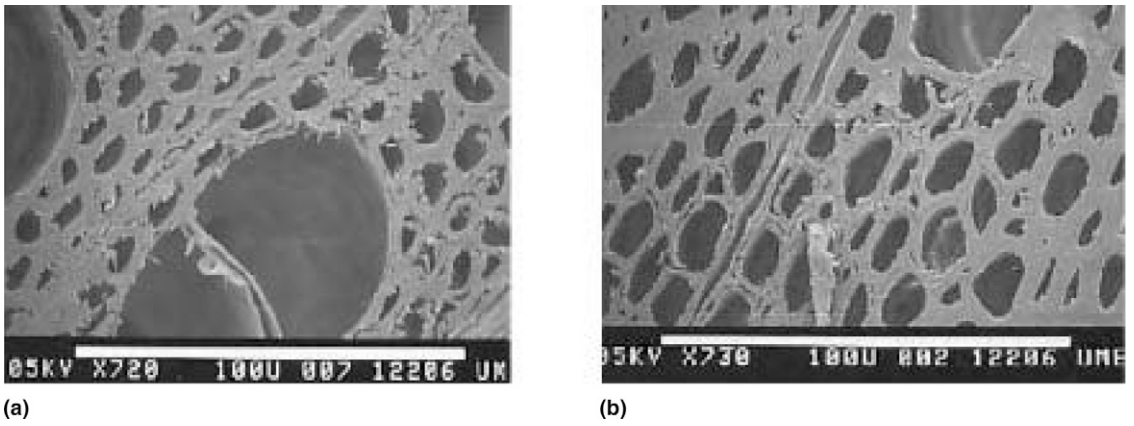


Figure 3. Cross-sectional views of (a) red maple control specimens and (b) extracted red maple (SF = 3.81). Scale bar = 100 μ m. SF = severity factor.

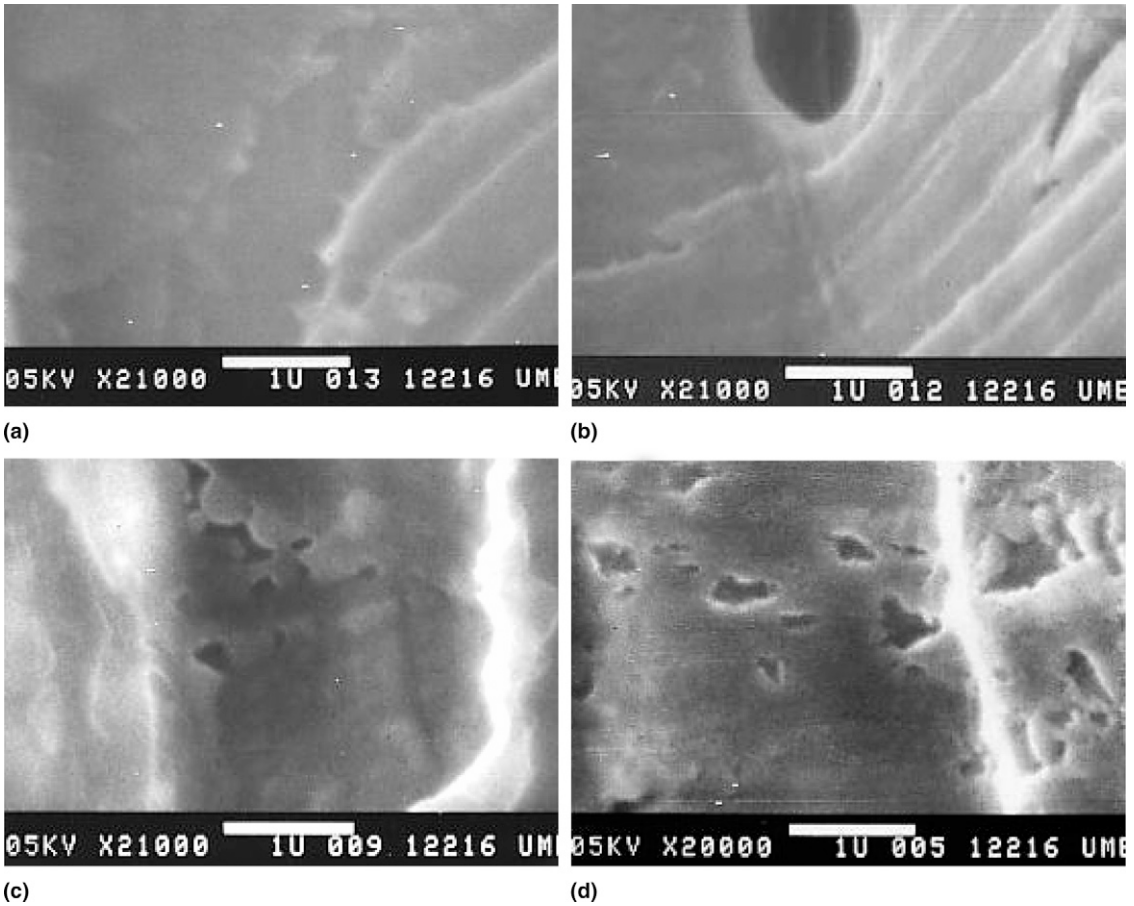


Figure 4. Transverse section views of red maple strands for (a) unextracted condition (SF 0), (b) SF 2.71, (c) SF 3.54, and (d) SF 3.81, which illustrate progressive cell-wall damage. Scale bar = 1 μ m. SF = severity factor.

will not penetrate pores by capillary action (Washburn 1921). Moura et al (2005) defined two ranges of porosity as: 1) surface porosity, pores in the range of 10 – 100 μm , which represent lumens of vessels and fibers; and 2) internal porosity, pores in the range 0.1 – 10 μm , which is related to pits and openings in the wood cell wall.

In this experiment, the normalized mercury intrusion volume, which is related to void volume, was 58.9, 58.8, 81.3, and 76.7% for control, SF 2.71, SF 3.54, and SF 3.81, respectively. The average void volume of the extracted material (SF 3.54 and SF 3.81) was 22.4% more than the void volume of the control as a result of extraction (Fig 5), whereas that between the control and SF 2.71 was not significantly different. Between a pore diameter of 0.6 and 0.3 μm , the void volume of the SF 3.54 and SF 3.81 increased and was greater than the control and SF 2.8 materials, implying that the extraction time was responsible for the largest apertures in that porosity range. Additionally, it indicated that internal porosity was greater than surface porosity. The SF 3.81 condition had less void volume and smaller pore size than SF 3.54 material. This result is hypothesized to be related to changes in the cellulose microfibril organization in accordance with the microfibril width changes determined by X-ray diffraction. Moura et al (2005) had similar results of total porosity 79.1 and 47.6% for control and treated wood, respectively. The wood chips were

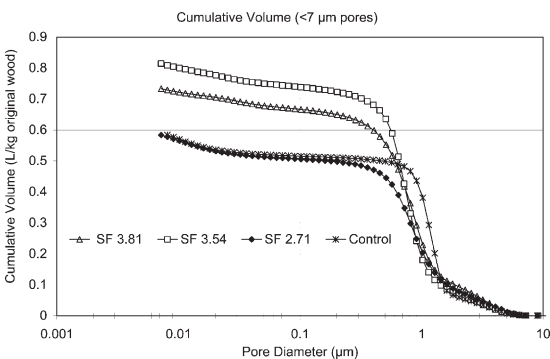


Figure 5. Cumulative volume distribution (less than 7 μm pores) of red maple strands as a function of severity factor.

cooked at 160°C in a digester with water, 16% Na_2O , and 30% sulphidity. In addition, Grioui et al (2007) investigated the porosity changes by carbonization of wood in a temperature range between 200 and 350°C by mercury porosimetry and environmental SEM. The total porosity of carbonized wood in an inert atmosphere increased as the temperature increased, which was attributed to the cracking of the cell wall and the degradation of hemicelluloses, cellulose, and lignin.

Crystallinity

Changes in the supermolecular structure of the respective polymorph forms of cellulose for the control and three SF specimens were analyzed as a function of the extraction conditions (Fig 6). The determined percentage crystallinity values were 51.3 ± 3.3 , 55.7 ± 3.6 , 61.7 ± 3.9 , and $59.5 \pm 4.1\%$ for the control, SF 2.71, SF 3.54, and SF 3.81, respectively. The percentage of crystallinity was significantly influenced by extraction conditions ($p = 0.0319$). No statistically significant difference between the noncontrol treatments was indicated by a Bonferroni multiple comparison at the 95% confidence level.

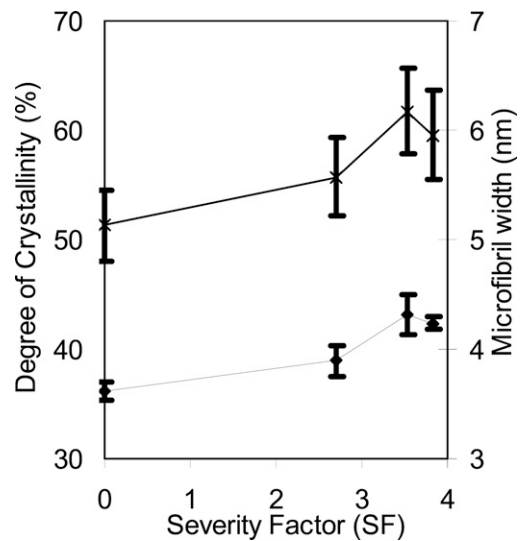


Figure 6. Graph shows the degree of crystallinity and microfibril width as a function of severity factor.

Crystallite width varied in a similar manner as percentage crystallinity, 3.61 ± 0.08 , 3.89 ± 0.14 , 4.32 ± 0.19 , and 4.23 ± 0.06 nm for the control, SF 2.71, SF 3.54, and SF 3.81, respectively, again with no significant difference ($p = 0.5114$) between the high SF conditions. Similar trends, initial increases followed by decreases, have been observed in other wood species under hydrothermal conditions (Hirai et al 1972; Bhuiyan et al 2000; Akgül et al 2007) and wood degraded by fungi (Howell et al 2008). The changes in crystallinity were explained as crystallization in quasicrystalline or subcrystalline structures found by Ding and Himmel (2006) attributed to rearrangement or reorientation of cellulose molecules and hemicelluloses rather than loss of amorphous material (Bhuiyan et al 2000). Increases in the crystallite width of extracted wood indicated a swelling process resulting from application of hot water. Sarko and Muggli (1974) applied sodium to microfibrils of cellulose, which caused an increase in width as a result of a swelling process. Also, a reorientation process (Hill 2006) that can cause fiber aggregation through the removal of hemicelluloses may be taking place (Emons 1988).

Contact Angle

The development of a good adhesive bond requires the spreading, wetting, and penetration of an adhesive into the adherent (substrate). A common measure of wetting is contact angle, which indicates the wettability of a solid surface by a liquid. The contact angles formed can be used to determine the surface energy of the solid (Pocius 2002). Contact angles from the sessile drop experiment are shown in Table 1.

The contact angle formed by all the liquids excluding the control (distilled water, diiodomethane, and ethylene glycol) was less than 90° ; therefore, the liquids were able to penetrate the porous wood. In both SF 3.54 and 3.81 conditions, the contact angle determined using diiodomethane exhibited the fastest penetration into the strand. The SF 2.71 had a larger contact angle than the control. Complete penetration of the liquid into the wood occurred within a few seconds. The penetration of liquids into the wood structures is initialized by penetration of the gross capillary structure, lumens, and intercellular pits followed by movement into the spaces within the secondary wall. The mercury porosimetry study showed that the more severe extraction conditions (SF 3.54 and 3.81) had a higher pore volume. This translates to increased permeability and is consistent with the more rapid liquid penetration of the material. The process of manufacturing OSB depends on a good adhesive bond, typically using a polymeric diphenylmethane diisocyanate (pMDI) or phenol-formaldehyde resin systems. Generally, pMDI represents as little as 2% of dry furnish weight (Kamke and Lee 2007). The bondlines within OSB are discontinuous and the thickness is irregular because the OSB strands are not completely covered with resin (Conrad et al 2004). The increased permeability of the extracted material may have resulted in overpenetration of resin in the extracted strands, thereby contributing to the reduction in IB reported by Paredes et al (2008).

Surface Energy

Values of DN and AN* were found in the literature for the probes used in IGC (Table 2). The Schultz method was used for the

Table 1. Influence of hot water extraction on contact angle (degrees) after 3 s by the sessile drop method for three liquids.

Liquids	Control	SF 2.71	SF 3.54	SF 3.81
	Degrees			
Diiodomethane	13.9 ± 1.8	22.3 ± 5.6	0.0 ± 0.0	0.0 ± 0.0
Water	97.5 ± 3.1	0.0 ± 0.0	0.0 ± 0.0	0.0 ± 0.0
Ethylene glycol	0.0 ± 0.0	0.0 ± 0.0	0.0 ± 0.0	0.0 ± 0.0

SF = severity factor.

Table 2. Physical constants for probes used in inverse gas chromatography experiments.^a

Probe	Polarizability index $\alpha_0(\text{hu})^{0.5} \times 10^{49} \text{ C}^{3/2} \text{ m}^2 \text{ V}^{-1/2}$	DN Kcal/mole	AN* Kcal/mole	Specific characteristic
n-Octane	11.4	—	—	Nonpolar
n-Nonane	12.5	—	—	Nonpolar
n-Decane ^b	13.6	—	—	Nonpolar
n-Undecane ^b	14.7	—	—	Nonpolar
Acetone	5.8	17	2.5	Amphoteric
Chloroform	7.8	—	4.8	Acidic
Tetrahydrofuran	6.8	20	0.5	Basic
Ethyl acetate	7.9	17.1	1.5	Amphoteric

^a Park and Donnet 1998.

^b The values were calculated by extrapolation as Donnet and Balard (1991) did for n-Nonane in their original work.

DN and AN are the acceptor and donator numbers related to chemical

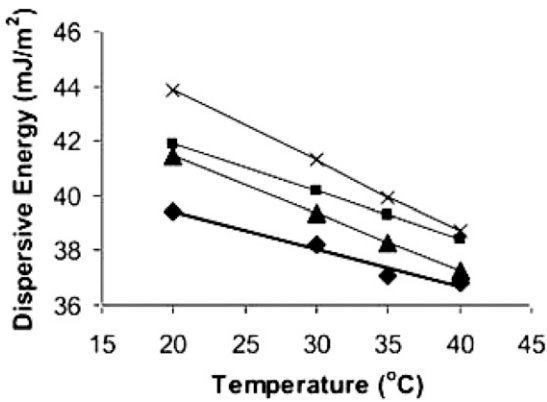


Figure 7. Dispersive surface energy calculated by the Schultz method for extracted red maple residues. ◆ is control, ■ is SF 2.71, ▲ is SF 3.54, and × is SF 3.81. SF = severity factor.

determination of the dispersive surface energy of the red maple samples. The results indicate that as more hemicelluloses are removed from the surface, there is an increase in surface energy of the wood (Fig 7). The control was not extracted and exhibited the lowest dispersive energy for the samples run. These results indicate that the surfaces of the red maple samples are impacted by the presence of extractives and the hemicellulose–lignin complex (Jara et al 2006). If this is the case, the acid and/or base characteristics of the red maple surface should increase with the removal of extractives. The polarization method proposed by Donnet and Balard (1991) was used to determine the acid/base, Ka, and Kb characteristics of the red maple samples (Fig 8). As SF increased, both Ka and Kb of the material increased; however, Kb had the largest increase

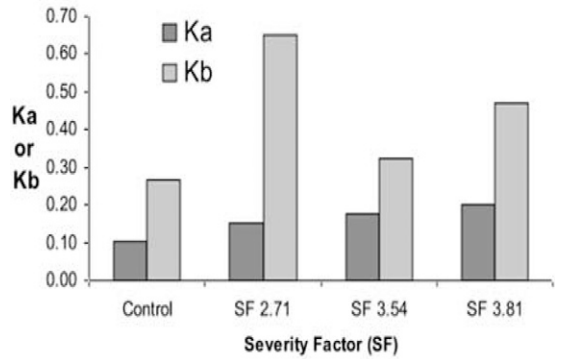


Figure 8. Ka and Kb calculated by the polarization method for extracted red maple residues.

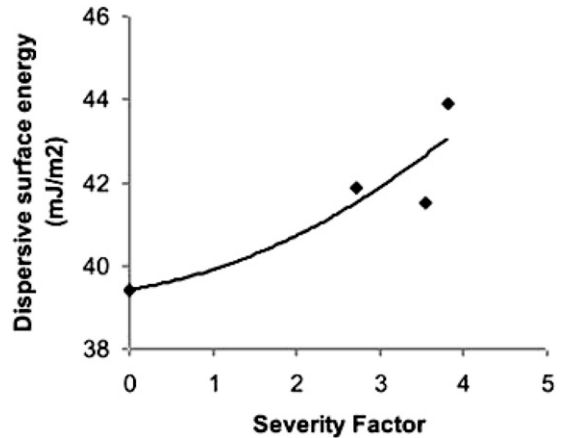


Figure 9. Dispersive surface energy (DSE) as a function of severity factor (SF); the polynomial equation for the curve was adjusted a quadratic regression, $DSE = 0.1715 SF^2 + 0.3073 SF + 39.425$ with a coefficient of determination, r^2 , of 0.8.

at SF 2.71 indicating that in the first step of extraction, the wood surface has a greater basic characteristic. The basicity is reduced as SF increases as a result of the presence of acid from cleavage of acetate groups from hemicellulose. This supports the conclusion that the removal of extractives exposes high-energy functional groups. In Fig 9, the severity factor is plotted vs the dispersive surface energy found by IGC and a correlation is observed. These findings suggest that the surface energy increases with extractive removal, and both acidic and basic functional groups are exposed.

CONCLUSIONS

The effect of extracted hot water extraction on adhesion-related characteristics of OSB strands was studied. Cell-wall damage was shown to occur as evidenced by pores. The extent of the pores increased as the extraction severity conditions increased from SF 3.54 to 3.81. Weight loss was correlated with up to 22.2% higher cell-wall pore volume with the increase primarily occurring at pore diameters between 0.8 and 3.0 μm . Little difference in the intracell-wall void structure was apparent below 0.8 μm for the SF 2.71 treatment. The crystallinity and width of cellulose increased as SF increased as a result of the reorientation of cellulose molecules as influenced by temperature, water, pressure, and extraction time. Sessile drop contact angle measurement on extracted wood strands showed rapid penetration of probe liquids. Hot water extraction increases the dispersive surface energy, acid base characteristics, and crystallinity of the red maple samples examined in this study. The reduction in IB of OSB manufactured from extracted strands is likely the result of the over-penetration of resin in the extracted strands caused by an increase in the porosity and permeability of wood as a result of the mass loss. For this reason, the recommended extraction procedure for red maple should be below SF 3.54.

ACKNOWLEDGMENTS

This material is based on work supported by the National Science Foundation under Grant

No. 0554545, "Investing in Maine Research Infrastructure; Sustainable Forest Bioproducts," the Department of Energy (Grant No. DE-FG36-04GO14246): Utilization of Pulp Mill Residuals, and the Maine Agricultural and Forest Experiment Station (MAFES). This is MAFES publication number 3029. Also contributing in this research were Professor Douglas Bousfield and Russell Edgar, MSc.

REFERENCES

- Akgül M, Gümüşkaya E, Korkut S (2007) Crystalline structure of heat-treated scots pine (*Pinus sylvestris* L.) and uludag fir (*Abies nordmanniana*, subsp. *bornmuelleriana*) wood. *Wood Sci Technol* 41(3):281 – 289.
- Akiyoshi K, Deguchi S, Yamaguchi N, Sunamoto J (1993) Self-aggregates of hydrophobized polysaccharides in water. Formation and characteristics of nanoparticles. *Macromolecules* 26(12):3062 – 3068.
- Badger PC (2002) Ethanol from cellulose: A general review. In J Janick and A Whipkey, eds. *Trends in new crops and new uses*. ASHS Press, Alexandria, VA. 10 pp.
- Bengtsson C, Jermer J, Clang A, Ek-Olausson B (2003) Investigation of some technical properties of heat-treated wood. International Research Group on Wood Protection, IRG/WP 03-40266.
- Bhuiyan MTR, Hirai N, Sobue N (2000) Changes of crystallinity of wood cellulose by heat treatment under dried and moisture conditions. *J Wood Sci* 46(6):431 – 436.
- Blankenhorn PR, Barnes DP, Kline DE, Murphey WK (1978) Porosity and pore size distribution of Black cherry carbonized in an inert atmosphere. *Wood Sci* 11(1):23 – 29.
- Borrega M, Karenlampi P (2008) Effect of relative humidity on thermal degradation of Norway spruce (*Picea abies*) wood. *J Wood Sci* 54(4):323 – 328.
- Carrasco F, Roy C (1992) Kinetic study of dilute-acid prehydrolysis of xylan-containing biomass. *Wood Sci Technol* 26(3):189 – 208.
- Cochin D, de Schryver FC, Laschewsky A, van Stam J (2001) Polysoaps in aqueous solutions: Intermolecular versus intramolecular hydrophobic aggregation studied by fluorescence spectroscopy. *Langmuir* 17(9):2579 – 2584.
- Conrad MPC, Smith GD, Fernlund G (2004) Fracture of wood composites and wood-adhesive joints: A comparative review. *Wood Fiber Sci* 36(1):26-39.
- Dahlman O, Tomani P, Axegard P, Lundqvist F, Londgren K (2007) Method for separating polymeric pentose from a liquid/slurry. World Intellectual Property Organization (WIPO), International Publication Number WO 2007/120091 A1.

- Ding SY, Himmel ME (2006) The maize primary cell wall microfibril: A new model derived from direct visualization. *J Agric Food Chem* 54(3):597 – 606.
- Donnet JB, Balard H (1991) Surface characteristics of pitch-based carbon-fiber by inverse gas-chromatography. *Carbon* 29(7):955 – 961.
- Emons AMC (1988) Methods for visualizing cell-wall texture. *Acta Bot Neerl* 37(1):31 – 38.
- Falkehag SI (1975) Chemical and electron microcopy studies on carefully isolated softwood lignin. *Holzforchung* 30(1):1 – 6.
- Fengel D, Wegener G (1984) *Wood: Chemistry, ultrastructure, reaction*. Walter de Gruyter, Berlin, Germany. 613 pp.
- Fujita Y, Takahashi S, Ueda M, Tanaka A, Okada H, Morikawa Y, Kawaguchi T, Arai M, Fukuda H, Kondo A (2002) Direct and efficient production of ethanol from cellulosic material with a yeast strain displaying cellulolytic enzymes. *Appl Environ Microbiol* 68(10): 5136 – 5141.
- Gardner DJ, Generalla NC, Gunnells DW, Wolcott DJ (1991) Dynamic wettability of wood. *Langmuir* 7 (11):2498 – 2502.
- Garrote G, Dominguez H, Parajo JC (1999) Hydrothermal processing of lignocellulosic materials. *Holz Roh Werkst* 57(3):191 – 202.
- Grioui N, Halouani K, Zoulalian A, Halouani F (2007) Experimental study of thermal effect on olive wood porous structure during carbonization. *Madera Ciencia y Tecnologia* 9(1):15 – 28.
- Hill C (2006) *Wood modification: Chemical, thermal, and other processes*. John Wiley & Sons Series in Renewable Resources, Hoboken, NJ. 239 pp.
- Hirai N, Sobu EN, Asano I (1972) Studies on piezoelectric effect of wood. IV. Effects of heat treatment on cellulose crystallites and piezoelectric effect of wood. *Mokuzai Gakkaishi* 18(11):535 – 542.
- Howell C, Paredes J, Shaler SM, Jellison J (2008) Decay resistance properties of hemicellulose-extracted oriented strand board. International Research Group on Wood Protection, IRG/WP 08-10644.
- , Steenkjaer AC, Jellison J (2007) The use of X-ray diffraction for analyzing biomodification of crystalline cellulose by wood decay fungi. International Research Group on Wood Protection, IRG/WP 07-10622.
- ISO/AWI (2004) Pore size distribution and porosimetry of material-evaluation by mercury porosimetry. ISO/AWI 15901-1. London. Pages 1 – 4.
- Jara R, Paredes JJ, van Heiningen A, Shaler SM (2006) Influence of hemicelluloses extraction on suitability for oriented strand board (OSB) production–extraction study. Presented at First Conference on Biorefineries, Univ. de Concepcion, Concepcion, Chile.
- Jeoh T (1998) Steam explosion pretreatment of cotton gin waste for fuel ethanol production. MS Thesis, Virginia Polytechnic Institute. Pages 27 – 46.
- Kamke FA, Lee JN (2007) Adhesive penetration in wood: A review. *Wood Fiber Sci* 39(2):205 – 220.
- Klose W, Schinkel A (2002) Measurement and modeling of the development of pore size distribution of wood during pyrolysis. *Fuel Process Technol* 77 – 78(1):459 – 466.
- Lavielle L, Schultz J (1991) Surface-properties of carbon-fibers determined by inverse gas-chromatography—Role of pretreatment. *Langmuir* 7(5):978 – 981.
- Lawoko M, Berggren R, Berthold F, Henriksson G, Gellerstedt G (2004) Changes in the lignincarbohydrate complex in softwood kraft pulp during kraft and oxygen delignification. *Holzforchung* 58(6):603 – 610.
- Lora JH, Wayman M (1980) Autohydrolysis of aspen milled wood lignin. *Can J Chem* 58(7):669 – 676.
- Lee S, Shupe TF, Groom LH, Hs ECY (2007) Wetting behaviors of phenol- and urea-formaldehyde resins as compatibilizers. *Wood Fiber Sci* 39(3):482 – 492.
- Mao H, Genco JM, van Heiningen A, Pendse H (2008) Technical economic evaluation of a hardwood biorefinery using the ‘near-neutral’ hemicellulose pre-extraction process. *J Biobased Materials and Bioenergy* 2(2): 177 – 185.
- McDonald AG, Clare AB, Meder AR (1999) Chemical characterisation of the neutral water soluble components from radiata pine high temperature TMP fibre. Volume 2. Pages 641 – 647 in Proc. 53rd General APPITA Conference, 19–22 April 1999, Rotorua, New Zealand.
- , Fernandez M, Kreber B, Laytner F (2000) The chemical nature of kiln brown stain in radiata pine. *Holzforchung* 54(1):12 – 22.
- Mills RH, Tze WTY, Gardner DJ, van Heiningen A (2008) Inverse gas chromatography for the determination of the dispersive surface free energy and acid–base interactions of a sheet molding compound I. Matrix material and glass. *J Appl Polym Sci* 109(6):3519 – 3524.
- Mitchell PH (1988) Irreversible property changes of small loblolly pine specimens heated in air, nitrogen, or oxygen. *Wood Fiber Sci* 20(3):320 – 335.
- Mosier N, Ladisch C, Ladisch M (2002) Characterization of acid catalytic domains for cellulose hydrolysis and glucose degradation. *Biotechnol Bioeng* 79(6):610 – 618.
- Moura MJ, Ferreira PJ, Figueiredo MM (2005) Mercury intrusion porosimetry in pulp, and paper technology. *Powder Technol* 160(2):61 – 148.
- Norgren M, Edlund H, Wågberg L (2002) Aggregation of lignin derivatives under alkaline condition. Kinetics and aggregate structure. *Langmuir* 18(7):2859 – 2865.
- Overend RP, Chornet E (1987) Fractionation of lignocellulosic by steam-aqueous pretreatments. *Philos Tr R Soc A* 321(1561):523 – 536.
- Paredes JJ, Jara R, van Heiningen A, Shaler SM (2008) Influence of hemicellulose extraction on physical and mechanical behavior of OSB. *Forest Prod J* 58(12) (in press).
- Park SJ, Donnet JB (1998) Anodic surface treatment on carbon fibers: Determination of acid-base interaction parameter between two unidentical solid surfaces in a composite system. *J Colloid Interf Sci* 206(1):29 – 32.

- Pocius AV (2002) Adhesion and adhesives technology: An introduction. Hanser/Gardner Publ Inc, Cincinnati, OH. 319 pp.
- Sarko A, Muggli R (1974) Packing analysis of carbohydrates and polysaccharides III. Valonia cellulose and cellulose III. *Macromolecules* 7(4):486 – 494.
- Seborg RM, Tarkow H, Stamm AJ (1953) Effect of heat upon the dimensional stabilization of wood. *J Forest Prod Res Soc* 3(3):59 – 67.
- Sjöström E (1993) Wood chemistry: Fundamentals and applications. 2nd ed. Laboratory of Wood Chemistry, Forest Products Department, Helsinki Univ. of Techn., Espoo, Finland. 223 pp.
- Stamm AJ, Burr HK, Kline AA (1946) Staywood. Heat-stabilized wood. *Ind Eng Chem* 38(6):630 – 634.
- Sundqvist B, Karlsson O, Westermark U (2006) Determination of formic-acid and acetic acid concentrations formed during hydrothermal treatment of birch wood and its relation to colour, strength and hardness. *Wood Sci Technol* 40(7):549 – 561.
- , Morén T (2002) The influence of wood polymers and extractives on wood colour induced by hydrothermal treatment. *Holz Roh Werkst* 60(5):375 – 376.
- Varga D, van der Zee ME (2008) Influence of steaming on selected wood properties of four hardwood species. *Holz Roh Werkst* 66:11 – 18.
- Washburn EW (1921) The dynamics of capillary flow. *Phys Rev* 17(3):273 – 283.
- Westbye P, Köhnke T, Glasser W, Gatenholm P (2007) The influence of lignin on the self-assembly behaviour of xylan rich fractions from birch (*Betula pendula*). *Cellulose* 14(6):603 – 613.
- Wood CD, Amidon TE, Liu S (2008) Membrane separation of hardwood autohydrolysis extracts for production of bio-based chemicals and fuels. Pages B457 – B462 in 94th Annual Meeting, Pulp and Paper Technical Association of Canada (PAPTAC), 4–7 February 2008, Montreal, Quebec, Canada.
- Yoon SH, Macewan K, van Heinigen A (2006) Pre-extraction of southern pine chips with hot water followed by kraft cooking. Page 157 in TAPPI Engineering, Pulping, & Environmental Conference, 5 November 2006, Atlanta, GA.